

Optimization of Transient Response Radiation of Printed Ultra Wideband Dipole Antennas (Using Particle Swarm Optimization Method)

Petr ČERNÝ, Miloš MAZÁNEK

Dept. of Electromagnetic Field, Czech Technical University, Technická 2, 166 27 Praha, Czech Republic

xcernyp1@fel.cvut.cz, mazanekm@fel.cvut.cz

Abstract. *In case of particular ultra wideband applications (i.e. radar, positioning, etc.), it is crucial to know the transient responses of antennas. In the first part of the paper, the optimization process searches for the dipole shape that accomplishes two required parameters i.e. a good matching and a minimal distortion. The particle swarm optimization method was used in the process of the dipole shape optimization. As a result, the optimized ultra wideband dipole is perfectly matched. Moreover, it minimally distorts the applied signal. The second part of the paper discusses the influence of the feeding circuit on radiating parameters and on the dipole antenna matching.*

Keywords

Ultra wideband antennas, UWB, particle swarm optimization, PSO, transient response radiation, dipole feeding.

1. Introduction

The ultra wideband (UWB) radio represents an emerging technology that attracts attention of both, industry and academia. An antenna represents the indispensable component of every radio system. Consequently, in this paper, the antenna is studied from the pulse radiation point of view. Firstly, the required ultra wideband antenna should be perfectly matched to the feeding line. Secondly, it could serve as a Gaussian impulse-shaping filter and, at the same time, radiate impulses similar to the higher orders of the Gaussian impulses.

1.1 Ultra Wideband Technology

The ultra wideband technology is defined as any radio technology using signals that have a spectrum occupying a bandwidth either greater than 20 % of the centre frequency or a bandwidth greater than 500 MHz, see [1]. This represents the main difference from the narrow band technologies whose bandwidth typically does not exceed 10 % of the centre frequency.

European Telecommunications Standards Institute (ETSI) and US Federal Communications Commission (FCC) defined the frequency mask, which determines the maximal radiated power of the ultra wideband signal. This mask indicates the frequency band ranging from 3.1 to 10.6 GHz within which the ultra wideband signal is transmitted with a maximum power. For the ultra wideband signals, the first derivative (or higher) of the Gaussian impulse is mostly used.

1.2 UWB Antennas and Parameters

The ultra wideband antennas with a flat amplitude and a linear phase of the transmission coefficient radiate the applied impulse without any distortion. These antennas are predominantly directional and could be used as measurement antennas. To give an example of such type of antenna, we can mention the Vivaldi antenna, whose fidelity of radiated and applied impulse is very high (0.969, see [2]). However, the key advantage of the planar dipoles is represented by the fact that they have omni-directional radiation patterns, substantially smaller dimensions and turn out to be more suitable for any communication devices, radars, positioning devices, etc. Moreover, the dipole antennas derivate the applied signal at the antenna port, [3], [4]. Basic shapes of wideband dipoles, such as elliptical, diamond and thick, are discussed in [3], [4], [5].

In this paper, the optimization process searches for the dipole shape, which meets the required parameters, i.e. a good matching and a minimal distortion of radiated impulses.

2. Dipole Shape Optimization Procedure Using PSO

The implementation of the optimization procedures contains the optimization function, the evaluating function, the start conditions, the object of optimization and its parameterization. The entire optimization process is implemented in MATLAB[®] except for the part of the evaluation function, which solves the simulated structure in the full-

wave electromagnetic field simulator CST Microwave Studio®.

The discretization of the dipole structure is carried out by the following parameters: the dipole element length by L , the shape by w_0-w_{20} and the dipole parts gap by s , see Fig. 1.

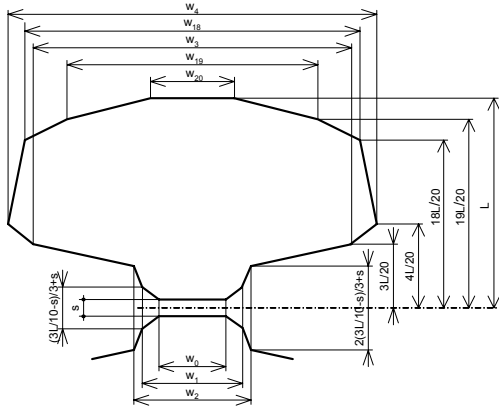


Fig. 1. Optimized dipole dimensions.

2.1 Particle Swarm Optimization Method

The particle swarm optimization (PSO) represents a robust stochastic evolutionary optimization method benefiting from the movement and intelligence of swarms, [6]. To clarify the philosophy of the technique, it is possible to give the following example: there is a swarm of bees in a field, where the bees are searching for a location with the highest density of flowers. The bees have no priori information about the field. Consequently, when looking for flowers, they start in random locations with random velocities. Every bee is capable of remembering the locations where it found the highest number of flowers. The swarm is also capable of remembering the location where the whole swarm found the highest density of flowers.

The swarm is initialized with 42 particles (bees) with the random positions x_n and the random velocities v_n in the solution space. After solving the evaluating function, the best positions of the whole swarm and of each particle are updated. Subsequently, the velocities and positions are updated using the equations Eq. (1) and Eq. (2). The optimization process is repeated except for the swarm initialization

$$v_{n+1} = w * v_n + c_1 * rand() * (p_{best,n} - x_n) + c_2 * rand() * (g_{best} - x_n), \quad (1)$$

$$x_{n+1} = x_n + \Delta t * v_n. \quad (2)$$

The evaluating of the fitting function consists of the updating of discretization parameters of the dipole structure, solving the transient analysis of the dipole structure in CST® and solving the fitting function (with the help of the

results obtained by CST®), [4]. The part of the fitting function that describes the distortion is evaluated as fidelity from the derivative of the excitation impulse with the radiated impulse. The excitation impulse is the second derivative of the Gaussian impulse, see Fig. 2. The part of the fitting function of the matching is evaluated as an average of numbers (at each frequency) between zero (for the reflection better then the required limit) and one (for the total reflection) within the required frequency band.

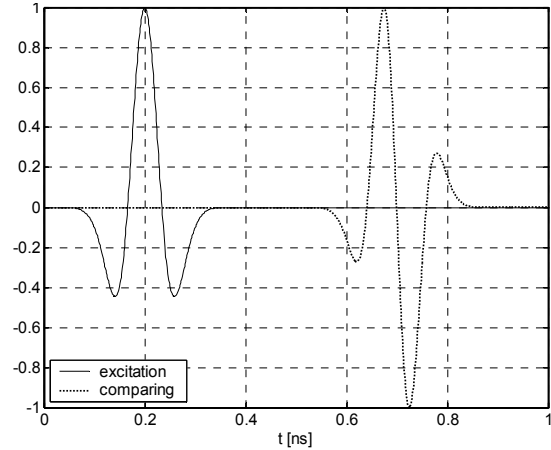


Fig. 2. Excitation impulse (solid, left) and impulse used in computing of fidelity (dashed, right).

2.2 Results of Dipole Shape Optimization Using PSO Method

The optimization process was carried out by means of the particle swarm optimization method. The result shape is shown in Fig. 3a. This serrated shape was manually smoothed, see Fig. 3b.

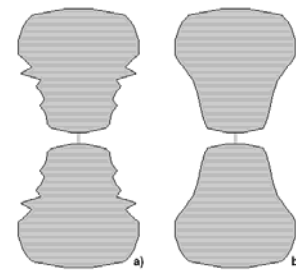


Fig. 3. Optimized dipole shapes, a) the original shape using PSO, b) the smoothed shape.

The values of the fitting functions are compared for the serrated (original) and the smoothed dipole shapes in Tab. 1. The simulations of these dipoles are performed with the 100 Ω non-physical feeding differential port. The reflection coefficients for both dipole shapes are depicted in Fig. 3. The radiated impulses to the normal direction are shown in Fig. 4 for both dipole shapes. Fig. 5 shows the radiated impulses that go with the original as well as the dipole shapes smoothed to the side direction.

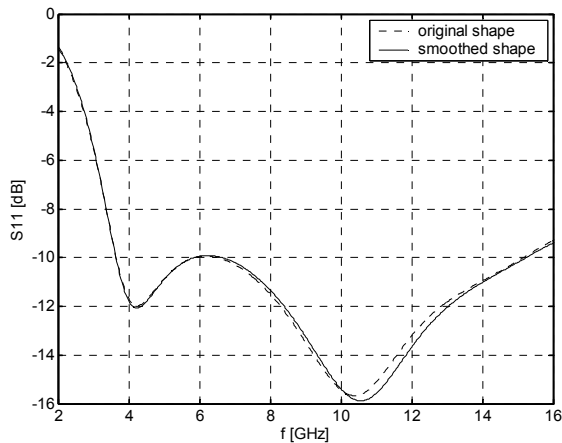


Fig. 4. Comparison of the reflection coefficient of the original dipole (dashed line) and the smoothed dipole (solid line).

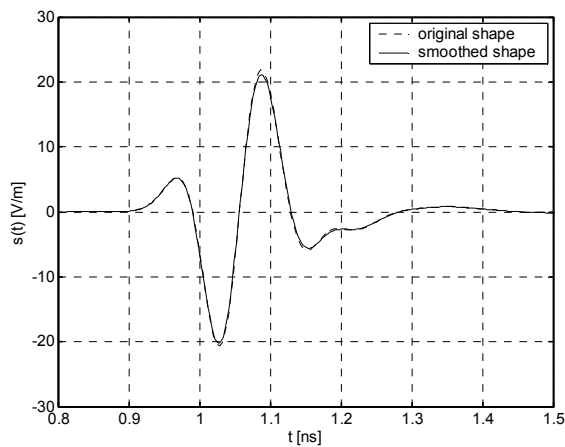


Fig. 5. Comparison of the radiated impulse to the side direction of the original dipole (dashed line) and the smoothed dipole (solid line).

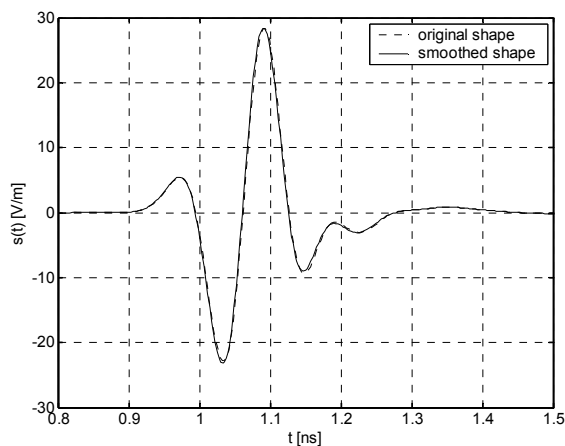


Fig. 6. Comparison of the radiated impulse to the normal direction of the original dipole (dashed line) and the smoothed dipole (solid line).

The obtained results are very similar and the difference between overall fitting functions equals approximately to 0.13 %. This very insignificant difference can be

seen from the comparison of the charts in Fig. 4 – 6. The matching coefficients are above -10 dB limit when the frequency is lower than 3.65 GHz. The matching is on the level of -6.1 dB on the frequency equal to 3.1 GHz. The radiated impulses are very similar to the third derivative of the Gaussian impulse and the distortion of these impulses is exactly expressed in the following table.

Fitting function	original shape	smoothed shape
Matching	0.9854	0.9850
Fidelity – side radiation	0.9457	0.9381
Fidelity – normal radiation	0.9624	0.9666

Tab. 1. Summarization of the results obtained by PSO method.

3. Dipoles with Real Feeding Circuits

The feeding circuit represents an indispensable part of all antennas and determines significantly antenna parameters. The differential feeding port used for the excitation of optimized dipoles in the previous chapter is a non-physical port and was used only for the simplification of the optimized structure and acceleration of the optimization process. On the other hand, it is necessary to feed the optimized structures by a circuit that would be more suitable and more satisfactory from the physical point of view. Two very different feeding circuits were used for the dipoles feeding. These methods were designed to be used in printed structures.

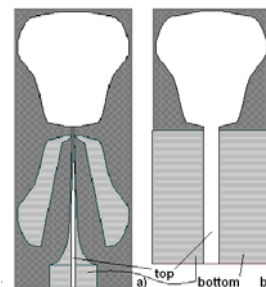


Fig. 7. Resulting structures with feeding circuits, a) dipole with balun transformer, b) monopole with planar ground plane.

In general, the dipoles have zero radiation in the direction of the dipole axis. Thus, the most suitable way to feed the dipole is to guide the feeding signal in the dipole axis. For the feeding of the optimized dipole structure, the 50 Ω microstrip line was used. In the first case, a feeding planar balun transformer progressively transforms from the impedance 50 Ω of the microstrip line to impedance 100 Ω of the parallel-plate line. This parallel plate line is directly connected to the feeding gap between the dipole parts. This solution avoids coupling between the radiation near-field around the dipole and between the feeding circuits. Commonly used feeding balun also reduces the dipole reflections and transforms the asymmetrical feeding line into the

symmetrical line. The resulting dipole structure together with the feeding balun transformer is depicted in Fig. 7a. A similar solution can be found in [5].

The second solution is based on feeding of the monopole directly by the 50Ω microstrip feeding line. The monopole element and the planar ground plane are situated on the same microwave substrate, but on opposite sides. The monopole ground plane is simultaneously the ground plane of the microstrip line. The gap between the monopole element and the ground plane is half as big as the dipole elements gap. The advantage of this solution is simplicity of the realization. But on the other hand, the reflection coefficient of this solution is very sensitive to the antenna mounting or holding. The different holding of the monopole antenna by the hand can make difference more than 5dB. The resulting monopole structure with planar ground plane is depicted in Fig. 7b. A similar solution can be found in [7].

3.1 Performances of Dipoles with Feeding Circuits – Simulation

The feeding parts of the dipole and monopole were tuned step-by-step in order to minimize the reflection coefficient in the required frequency band. The values of the fitting functions are compared for the dipole and the monopole structures in Tab. 2. The simulations of these dipoles are performed with the excitation by the waveguide port with the impedance equal to 50 Ω. The radiated impulses to the side direction are shown in Fig. 8 for both structures. The radiated impulses to the normal direction are shown in Fig. 9. The reflection coefficient for the dipole structures with the balun transformer is shown in Fig. 10. The reflection coefficient for monopole structures with the planar ground plane is depicted in Fig. 11.

Fitting function	dipole shape	monopole shape
Matching	0.8802	0.8113
Fidelity – side radiation	0.9435	0.9210
Fidelity – normal radiation up	0.9628	0.9680

Tab. 2. Summary of the obtained results of dipole or monopole antennas with feeding circuits.

The reflection coefficient of antennas for mobile devices is acceptable at the level of -6 dB. Antennas with perfect matching are more sensitive to the reflections on the touching by hand or by head. Reflections of the tuned dipole and monopole are better than the level of -7 dB. It is obvious that the mismatching at the level of -7 dB has an insignificant influence on the fidelity of the radiated impulses, in comparison to the previously optimized dipoles. The amplitudes of radiated impulses are lower in comparison to the previously optimized dipoles. The difference approximately amounts to 16 %. The time shift between impulses is caused by the different length of the feeding structures.

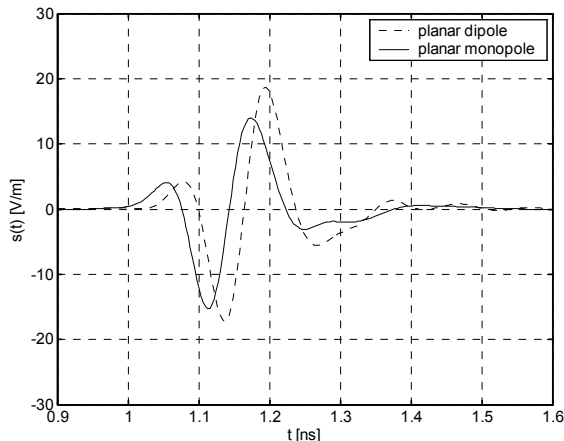


Fig. 8. Comparison of the radiated impulse to the side direction of the dipole structure with the balun transformer (dashed line) together with the monopole with the planar ground plane (solid line).

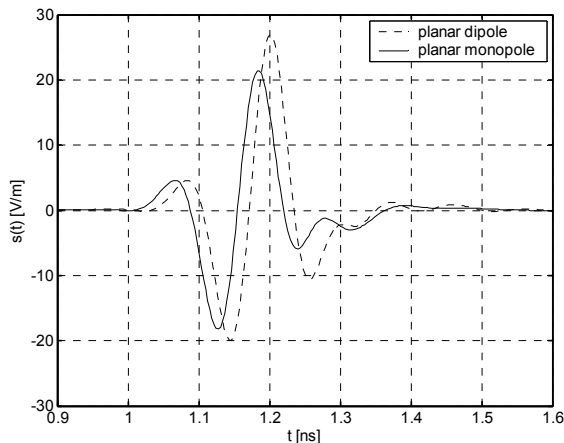


Fig. 9. Comparison of the radiated impulse to the normal direction of the dipole structure with the balun transformer (dashed line) together with the monopole with the planar ground plane (solid line).

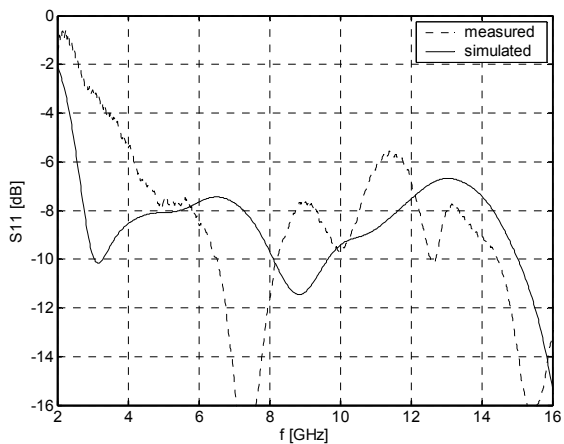


Fig. 10. Comparison of the reflection coefficient of the dipole with the balun transformer simulation (solid line) together with the dipole measurement (dashed line).

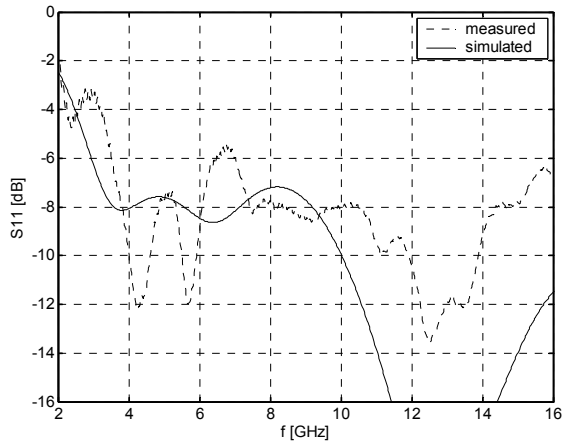


Fig. 11. Comparison of the reflection coefficient of the monopole with planar ground plane simulation (solid line) together with the monopole measurement (dashed line).

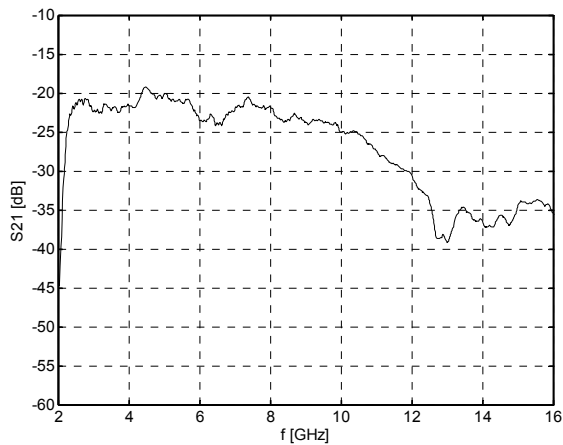


Fig. 12. Measurement of the transmission coefficient between the dipole with the balun transformer and the monopole with the planar ground plane – amplitude response.

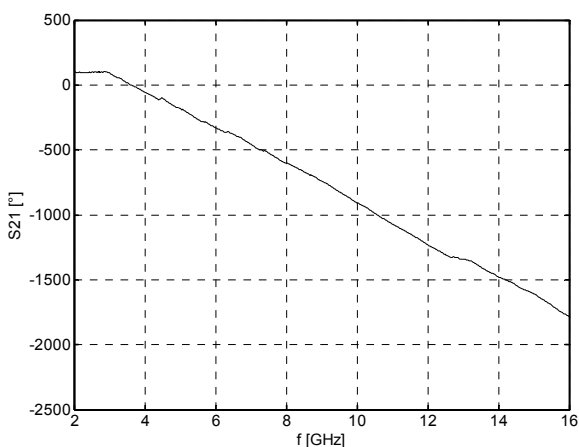


Fig. 13. Measurement of the transmission coefficient between the dipole with the balun transformer and the monopole with the planar ground plane – phase response.

3.2 Performances of Dipoles with Feeding Circuits – Measurement

The previously presented and tuned dipole with the balun transformer and the monopole with the planar ground plane antennas were manufactured and measured. In the Fig. 15 the manufactured antennas are presented. The comparison between the simulated and measured reflection coefficient in case of the dipole antenna is depicted in Fig. 10, while the one in case of the monopole antenna is shown in Fig. 11.

The differences between the measurement and simulation for the dipole and monopole antennas are significant. There are several factors that made rise to aforementioned disconformities. The key ones follow - the connector body, the discontinuities of the feeding connector as well as the feeding cable were not included in the antenna simulation.

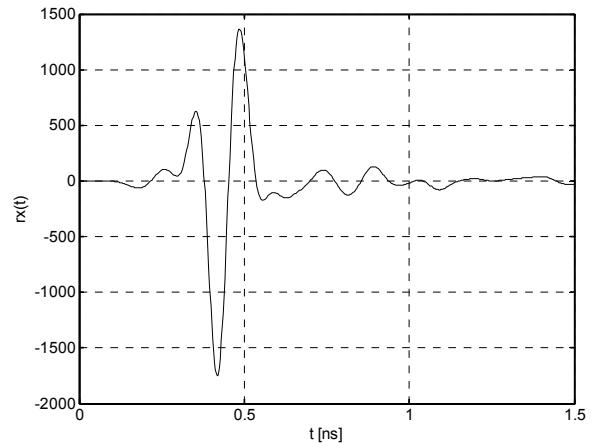


Fig. 14. Computed impulse transmission response between the dipole and monopole in case of planar monopole excitation carried out by the second derivative of Gaussian impulse.

Reflections are worse than the level of -7 dB, mainly at lower frequencies and around 11 GHz for the dipole antenna, respectively around 7 GHz for the monopole antenna. The amplitude response of the transmission coefficient between the dipole and the monopole antenna is depicted in Fig. 12. The amplitude response is flat in the range of ± 3 dB. The phase response of the transmission coefficient between the dipole and the monopole antenna is presented in Fig. 13. The phase response is flat and linear in the UWB frequency range with insignificant deviations. Furthermore, the computed impulse transmission response between the dipole and monopole antenna can be seen in Fig. 14. This impulse transmission response is obtained by the inverse Fourier transformation of the measured transmission coefficient to an impulse response. Moreover, the computed impulse transmission response, with the help of impulse response, is solved as the convolution with the excitation impulse (the second derivative of the Gaussian

impulse). The fidelity of the computed impulse transmission with the excitation impulse equals to 0.8587. The ringing around the main parts of the impulse transmission is caused mainly by the non-ideal flatness of the transmission coefficient amplitude response. But the main part of the impulse has substantially larger amplitude than the ringing, approximately ten times. On the other hand, the impulse transmission response has not the same transient response as the radiated impulse that has been discussed in the previous parts of the paper.

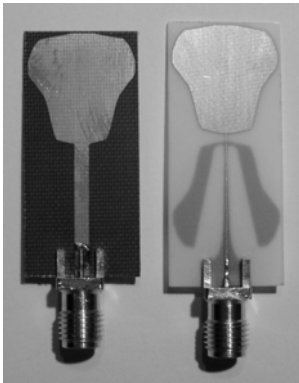


Fig. 15. Photography of realized dipole and monopole antennas.

4. Conclusion

The optimization using PSO method of the planar ultra wideband dipole shapes has been performed and its results have been presented and compared with the results obtained by the analysis of the dipole shape, whose shape was smoothed from the optimized shape. The optimized and smoothed dipole shapes offer very good performance, see Tab. 1.

The smoothed dipole shape was used as the radiating element for the dipole or monopole antennas expanded about the feeding circuits. In order to design the dipole antenna, the balun transformer was used. In case of the monopole antenna, the direct microstrip feeding line and the planar ground plane for the monopole were used.

These two antenna structures were analyzed, tuned and manufactured. The antennas are suitable for radiating and transmitting of the ultra wideband impulses, see results in Tab 2. The results of measurements confirm the very good impulse radiation performances of these antennas.

Acknowledgements

The research is a part of the activities of the Department of Electromagnetic Field of the Czech Technical

University in Prague in the frame of the research project of the Ministry of Education, Youth and Sports of the Czech Republic No. LC06071 Centre of quasi-optical systems and terahertz spectroscopy. The measurement was supported by the project Research in the Area of the Prospective Information and Navigation Technologies MSM 6840770014.

References

- [1] Federal Communications Commission, *First Order and Report, Revision of Part 15 of the Commission's Rules Regarding UWB Transmission Systems*, FCC 02-48, April 22, 2002.
- [2] PIKSA, P., SOKOL, V. Small Vivaldi antenna for UWB. In *Proceedings of the Conference RADIOELEKTRONIKA 2005*. Brno (Czech Republic), 2005, p. 490-493.
- [3] ČERNÝ, P., MAZÁNEK, M. Optimized ultra wideband dipole antenna. In *Proceedings of the 18th International Conference of Applied Electromagnetics and Communications*. Dubrovnik (Croatia), 2005.
- [4] ČERNÝ, P., MAZÁNEK, M., PIKSA, P., SOKOL, V., KOŘÍNEK, T. Transient response optimization of ultra wideband antennas (using particle swarm optimization). In *Proceedings of the European Conference on Antennas and Propagation*. Nice (France), 2006, p. 168.
- [5] SCHANTZ, H. G. Bottom fed planar elliptical UWB antennas. In *Proceedings of the Ultra Wideband Systems and Technologies*. Reston (USA), 2003, p. 219-223.
- [6] ROBINSON, J., RAHMAT-SAMII, Y. Particle swarm optimization in electromagnetics. *IEEE Transactions on Antennas and Propagation*, 2004, vol. 52, no. 2, p. 397-407.
- [7] KI-HAK KIM, YOUNG-JUN CHO, SOON-HO HWANG. Design of a Band-rejected UWB planar monopole antenna with two parasitic patches. In *Proceedings of the Conference ISAP2005*. Seoul (Korea), 2005, p. 957-960.

About Authors...

Petr ČERNÝ (*1976) received his M.Sc. degree from the Czech Technical University in Prague (CTU) in 2001. Now he is working on his Ph.D. thesis that is focused on the radio electronics. His research interest is in ultra wideband antennas and technology, measurement system and high-resolution terahertz spectroscopy. He is a member of IEEE.

Miloš MAZÁNEK (*1950) received his M.Sc and Ph.D. degrees from the CTU in 1974, and 1980 respectively. He has been a head of the Dept. of Electromagnetic Field (CTU) since 1997. He is a senior member of IEEE, the head of the Radioengineering Society and Radioengineering journal executive editor. His research interests are in the field of antennas, EMC, microwave radiometry and propagation.